HOKKAIDO UNIVERSITY

Title	Structural basis for pore-forming mechanism of staphylococcal α-hemolysin
Author(s)	Sugawara, Takaki; Yamashita, Daichi; Kato, Koji et al.
Citation	Toxicon, 108, 226-231 https://doi.org/10.1016/j.toxicon.2015.09.033
Issue Date	2015-12-15
Doc URL	https://hdl.handle.net/2115/63926
Rights	© 2015, Elsevier. Licensed under the Creative Commons Attribution-NonCommercial-NoDerivatives 4.0 International http://creativecommons.org/licenses/by-nc-nd/4.0/
Rights(URL)	https://creativecommons.org/licenses/by-nc-nd/4.0/
Type	journal article
File Information	Final_RevisedManuscript.pdf

Hokkaido University Collection of Scholarly and Academic Papers

Hokkaido University Collection of Scholarly and Academic Papers : HUSCAP

Structural basis for pore-forming mechanism of staphylococcal α-hemolysin

Takaki Sugawara[1], Daichi Yamashita[1], Koji Kato[1,2], Zhao Peng[3], Junki Ueda[3], Jun Kaneko[3], Yoshiyuki Kamio[3], Yoshikazu Tanaka[1,2*] , and Min Yao[1,2]

1. *Graduate School of Life Sciences, Hokkaido University, Sapporo, 060-0810, Japan.*
2. *Faculty of Advanced Life Sciences, Hokkaido University, Sapporo, 060-0810, Japan*
3. *Graduate School of Agricultural Science, Tohoku University, Sendai 981-8555, Japan*

[*]To whom correspondence should be addressed.

Tel. & Fax: +81-11-706-9017

E-mail: tanaka@sci.hokudai.ac.jp

Keywords: staphylococcal α-hemolysin, pore-forming toxin, crystal structure

Abstract

Staphylococcal α-hemolysin (α-HL) is a β-barrel pore-forming toxin (PFT) expressed by *Staphylococcus aureus*. α-HL is secreted as a water-soluble monomeric protein, which binds to target membranes and forms membrane-inserted heptameric pores. To explore the pore-forming mechanism of α-HL in detail, we determined the crystal structure of the α-HL monomer and prepore using H35A mutant and W179A/R200A mutant, respectively. Although the overall structure of the monomer was similar to that of other staphylococcal PFTs, a marked difference was observed in the N-terminal amino latch, which bent toward the prestem. Moreover, the prestem was fastened by the cap domain with a key hydrogen bond between Asp45 and Tyr118. Prepore structure showed that the transmembrane region is roughly formed with flexibility, although the upper half of the β-barrel is formed appropriately. Structure comparison among monomer, prepore and pore revealed a series of motions, in which the N-terminal amino latch released upon oligomerization destroys its own key hydrogen bond betweem Asp45–Try118. This action initiated the protrusion of the prestem. Y118F mutant and the N-terminal truncated mutant markedly decreased in the hemolytic activity, indicating the importance of the key hydrogen bond and the N-terminal amino latch on the pore formation. Based on these observations, we proposed a dynamic molecular mechanism of pore formation for α-HL.

35 ## Keywords

36 staphylococcal α-hemolysin, pore-forming toxin, crystal structure

37 ## Abbreviations

38 α-HL: α-hemolysin, PFT: pore-forming toxin

39

Highlights

- Crystal structures of the α-HL monomer and prepore were derermined.
- The prestem is fastened by a key hydrogen bond between Asp45 and Tyr118 in monomer.
- In prepore, the transmembrane region is roughly formed with flexibility.
- Upon oligomerization, the released amino latch destroys the key interaction to release prestem.
- A dynamic pore-forming mechanism, where the amino latch plays a key role, is proposed.

1. Introduction

Pathogenic bacteria secrete pore-forming toxins (PFTs) for attacking target cells. PFTs are secreted as water-soluble monomeric proteins, which assemble on the target cells for forming membrane-inserted pores. These pores then lead to cell death. PFTs are classified into two families according to the secondary structure of the transmembrane region, *i.e.*, α-PFTs and β-PFTs. *Staphylococcus aureus*, a major cause of hospital- and community-acquired infections, expresses several β-PFTs, including α-hemolysin (α-HL), γ-hemolysin (γ-HL), and leukocidin (LUK), for killing blood cells (Kaneko and Kamio, 2004). α-HL is a mono-component heptameric β-PFT, while the other two PFTs are bi-component octameric β-PFTs composed of two homologous polypeptides (~30% of amino acid sequence identity), designated as F and S components, respectively. α-HL reveals ~30% and ~20% sequence identity with F and S components, respectively.

Previous biochemical experiments have suggested a general pore-forming mechanism, in which the soluble monomeric components assemble into a ring-shaped pore via a nonlytic oligomeric intermediate known as a prepore (Kawate and Gouaux, 2003; Nguyen et al., 2002; Walker et al., 1995). However, the underlying mechanisms remain unelucidated because of the unavailability of the crystal structure of the α-HL monomer without an artificial binder and prepore. To explore this molecular process in detail, we determined the crystal structure of an H35A mutant (α-HL-H35A) and W179A/R200A mutant (α-HL-WR), which revealed monomeric and prepore form, respectively. Furthermore, mutation analysis was carried out. Based on these results, a dynamic mechanism of

α-HL assembly using hydrophobic interactions, in which the amino latch plays a key role, was proposed.

2. Materials and methods

2.1 Cloning, expression, and purification

The expression vector for mutants of α-HL was prepared by site-directed mutagenesis using the expression plasmid of wild-type α-HL as the template. In the resultant expression vector, a His_6-tag was fused at the C terminus of the toxin. Expression and purification of these mutants were performed as previously described (Sugawara et al., 2013; Tanaka et al., 2011). In brief, the *Escherichia coli* strain B834 (DE3) harboring the desired plasmid was grown at 37°C in LB medium containing 25 μg/mL of kanamycin. Isopropyl-β-D-thiogalactoside was added to obtain a final concentration of 0.5 mM when the optical density at 600 nm reached 0.6–0.8, followed by continuous culture for 24 h. The cells were collected and then disrupted by sonication in the sonication buffer (20 mM Tris-HCl, pH 8.0, and 200 mM NaCl). The α-HL mutants present in the supernatant were purified on a His-trap affinity column and a HiLoad 26/60 Superdex 200 column (GE Healthcare, Buckinghamshire, UK).

2.2 Crystallization, X-ray diffraction data collection, and structure determination

Crystals of α-HL-H35A suitable for further experiments were grown from a buffer containing 0.05 M sodium cacodylate (pH 6.5), 18 mM calcium chloride, 2.5 mM spermine, 9% (v/v) 2-propanol, and 5% (w/v) ethylene glycol. Crystals of α-HL-WR were grown from a buffer containing 40% MPD and 0.1 M citric acid (pH 4.0). X-ray diffraction experiments were performed at Photon Factory (Tsukuba, Japan) and SPring-8 (Harima, Japan) under proposals

90 2012G515/2014G022 and 2012A1179/2012B1215/2013A1115/2015A1117, respectively. Moreover,
91 X-ray diffraction dataset of α-HL-H35A and α-HL-WR was collected on the beamline BL5A and
92 BL17A at Photon Factory, respectively. The diffraction data were indexed, integrated, scaled, and
93 merged using the XDS program (Kabsch, 2010). The data statistics are shown in Table 1. Crystal
94 structures were determined by the molecular replacement method using the PHASER software
95 (McCoy et al., 2007). The structure of α-HL pore (PDB ID 3ANZ) was used as a search probe. To
96 monitor the refinement, a random 5% subset was set aside for the calculation of the R_{free} factor. After
97 rigid body refinement and manual model building with COOT (Emsley et al., 2010), individual
98 atomic coordinate refinement and individual ADP refinement were performed with phenix.refine
99 (Adams et al., 2010). The refinement statistics are summarized in Table 1. The atomic coordinates of
100 α-HL-H35A and α-HL-WR have been deposited in the Protein Data Bank, www.pdb.org (PDB ID
101 code 4YHD and 4P24, respectively).
102
103 *2.3 Assays of hemolytic activity and toxin binding to the rabbit erythrocytes.*
104 Aliquots of washed 1ml of 1% rabbit erythrocytes were incubated with 8 μg of α-HL or its
105 mutants at 37˚C for 30 min. After centrifugation, the supernatant was assayed for hemoglobin at 541
106 nm. Toxin binding to the rabbit erythrocyte membrane was analyzed by Western blotting with
107 anti-α-HL antiserum as described previously (Kaneko et al., 1997). For the detection of heptermar
108 complex, toxin treated rabbit erythrocyte membranes were solubilized with 1% SDS at 20 or 95˚C,

and then analyzed by Western blotting (Kaneko et al., 1997).

3. Results and discussion

3.1 Crystal structure of α -HL-H35A reveals key hydrogen bond between Asp45 and Try118

The substitution of His35 causes marked decreases in oligomerization and hemolysis activities and leads to an insufficient cell-binding activity (Walker and Bayley, 1995). As His35 is located at the interface between the protomers, this mutant is likely to retain the monomeric structure; however, in the absence of appropriate interprotomer interactions, it may not form heptamers. In the present study, we determined the crystal structure of α-HL-H35A mutants at a resolution of 2.80 Å.

As expected, the revealed structure was an α-HL monomer, in which the prestem was folded beside the cap domain (Fig. 1A). The prestem region, which is extended in the pore to form a β-barrel, was folded into a three-stranded antiparallel β-sheet with a long connecting loop in the monomer. Furthermore, a large conformational change was observed in the amino latch. Although the amino latch protrudes and interacts with the adjacent protomer in the pore, it is located at the edge of the β-sheet of the stem region. The tip of the amino latch forms a short helix in all known pore structures. However, this region had an extended conformation in the monomer.

The overall structure of the α-HL monomer was similar to that of other staphylococcal PFT monomers; RMSD was 1.30 Å for LukF, 1.14 Å for LukF-PV, 1.10 Å for LukD, 1.06Å for LukS-PV, and 0.91 Å for Hlg2. The folded prestem was fastened by a loop located at the top of the cap domain (hereafter loop-A (Yamashita et al., 2011), Yamashita et al. 2014). Asp45 of the loop-A formed a hydrogen bond with Tyr118 of prestem (Fig. 1B). A part of the long loop of the prestem (Thr129–

132 Gly134), involved in the formation of the transmembrane region of the pore, was disordered. These
133 structural characteristics are commonly observed in other staphylococcal PFT monomers.

134 In contrast to these common structural features, marked differences were observed in the
135 orientation of N-terminal amino latch and long connecting loop in the prestem (Fig. 1C). The amino
136 latch of the α-HL monomer bends toward the prestem, whereas it is aligned adjacent to the β-sheet in
137 other PFTs (Fig. 1C). Consequently, only a short β-strand was formed in this region of the α-HL
138 monomer. Two hydrophobic residues (Ile5 and Ile7) of the bent N-terminus amino latch form a
139 hydrophobic core with Phe39 located at the surface of the cap domain. This formation may supply
140 the driving force for the bent conformation of the amino latch. These residues are not conserved in
141 any other staphylococcal PFTs (Supplementary Fig. S1). Therefore, the hydrophobic core formation
142 is peculiar to α-HL, resulting in the characteristic bent conformation. As these structural
143 characteristics were common for all six α-HL monomers in an asymmetric unit, they are possibly the
144 intrinsic conformations of α-HL and not casual conformations because of flexibility.

145

146 *3.2 Crystal structure of α -HL-WR reveals two-step pore formatting mechanism*

147 The α-HL W179A/R200A double mutant (α-HL-WR) had no hemolytic activity, although
148 the binding activity for erythrocyte was comparable with the wild type (Fig. 2). Furthermore,
149 high-molecular weight complex on the rabbit erythrocyte membrane was observed by Western
150 blotting with low-temperature SDS-treatment (Fig. 2C). These observations suggest that α-HL-WR

151 forms stable prepore state oligomer. To acquire knowledge about prepore of α-HL, we determined
152 the crystal structure of this mutant in the presence of high concentration of MPD which induces
153 spontaneous heptameric assembly of α-HL (Tanaka et al., 2011). The revealed structure was quite
154 similar to that of α-HL pore (Fig. 3A). However, the electron density of the transmembrane region
155 was markedly ambiguous despite the clear density of the extramembrane half (Fig. 3B). The B-factor
156 of the transmembrane β-barrel is extraordinarily high (>100 $Å^2$) for this structure (Fig. 3A). These
157 observations suggest that the transmembrane region of α-HL-WR is roughly formed with flexibility,
158 although the upper half of the β-barrel is formed appropriately. This result is consistent with the
159 previously determined prepore structure of staphylococcal two-component PFTs, i.e. prepore and
160 pore is different in the flexibility of the transmembrane region, although other regions are quite
161 similar (Yamashita et al., 2014). Based on these observations, we consider the heptameric structure
162 of α-HL-WR as prepore of α-HL, hereafter. Due to the absence of Trp179 and Arg200 responsible
163 for the binding with the head group of phospholipid, the spontaneous pore formation of α-HL-WR
164 induced by MPD was likely to be incomplete, although their precise role on the β-barrel formation
165 was not clarified from crystal structure. For staphylococcal two-component PFTs, the two-step
166 pore-forming mechanism has been proposed, in which the upper part of the extramembrane domain
167 of the β-barrel is formed first, followed by the formation of the bottom transmembrane part of this
168 structure (Yamashita et al., 2014). The common propensity between the α-HL prepore and that of
169 two-component PFTs to form a flexible transmembrane region strongly suggests that the two-step

pore-forming mechanism is also applicable to α-HL.

3.3 Mechanism to release the prestem using the N-terminal amino latch

Our study presents the crystal structure of α-HL in the monomeric and oligomeric prepore states, enabling the description of a dynamic mechanism of α-HL assembly. Fig. 4A reveals the superposition of a monomer onto a protomer of the pore, which illustrates the motion of the released amino latch. The amino latch moves to the region previously occupied by the prestem. It is noteworthy that Asp13–Gly15 of amino latch in the pore occupies the position of Tyr118 in the monomer. Tyr118 is a key residue for fastening the prestem to the cap domain (Fig. 1B). These observations indicate that the released amino latch forces off the prestem by destroying the key interaction between the prestem and cap domain [*i.e.*, hydrogen bond Asp45–Try118 (Fig. 1B)].

To demonstrate the importance of the hydrogen bond between Asp45–Try118 and the amino latch, two mutants, i.e. Y118F mutant and truncate mutant of the N-terminal 14 residues (α-HL-ΔN14), were prepared and the hemolytic activity was measured (Fig. 2A). Both mutants dramatically decreased in the hemolytic activity. The binding activity of Y118F mutant for erythrocyte was also diminished markedly, whereas α-HL-ΔN14 possessed erythrocyte binding activity comparable with the wild type (Fig. 2B). The Y118F mutant is plausibly unable to hold the prestem stably in the monomeric state due to the disappearance of the key hydrogen bond, and the released prestem may inhibit stable binding to the erythrocyte membrane. Contrary to Y118F mutant,

189 the α-HL-ΔN14 could bind to erythrocytes but diminished its pore formation activity. α-HL-ΔN14 is
190 plausibly incapable to cleave the key hydrogen bond effectively because of the disappearance of the
191 N-terminal 14 residues. These result strongly supports the importance of physical contact in this
192 region.

193 Fig. 4B shows the superposition of two monomers on the two neighboring protomers of the
194 pore, representing the interaction between these monomers at the initial assembly step. A large steric
195 clash was observed between the amino latch of one protomer (shown in green in Fig. 4B) and the
196 prestem of the other (shown in red). The bent conformation of the amino latch, which is a structural
197 characteristic peculiar to α-HL, substantiates the degree of the steric clash. The bent amino latch
198 would be released by the steric repulsion when a monomer assembles with its adjacent protomer,
199 which would subsequently release the prestem itself because of the abovementioned physical contact.
200 Furthermore, the substitution of the α-HL amino latch with the amino latch of LukF, which had an
201 extended conformation, caused a drastic loss of hemolytic activity (Jayasinghe et al., 2006). This
202 report also indicates the importance of the steric repulsion of the amino latch owing to the bent
203 conformation. In addition to the steric hindrance between the amino latch and prestem, hindrances
204 between the prestems of the two protomers were also observed (red and yellow in Fig. 4B). This
205 phenomenon would also contribute to the release of the prestem.

206

207 *3.4 Hydrophobic interactions act as key role on pore formation*

In the monomer, the N-terminus amino latch had a characteristic bent conformation with the help of hydrophobic core formation using Ile5 and Ile7 of the amino latch and Phe39 located at the surface of the cap domain (Fig. 5A). In pore assembly, the amino latch protrudes and interacts with the adjacent protomer (Fig. 5B). During this conformational change, the N-terminus region of the amino latch folds into a short helix. This helix then forms a hydrophobic core with Ile14, Ile43, Leu52, Val54, and Val231 of the adjacent protomer, which stabilizes the conformation of the long protruded amino latch in the pore state (Fig. 5B). It is noteworthy that Ile5 and Ile7, important for the bent conformation of the amino latch in the monomer, re-participate in hydrophobic interactions. These two hydrophobic residues are important for the conformational conversion of the amino latch from monomer to oligomer. In the monomer, the prestem covers the hydrophobic surface of the cap domain, which binds to the N-terminal short helix. Further, the hydrophobic surface exposed by the release of prestem binds to the hydrophobic amino latch of the adjacent protomer in the pore. Altogether, α-HL efficiently uses the hydrophobicity of the amino latch for its structural conversion. Because of the stabilization of the protruded conformation in the pore, the amino latch may promote the cleavage of the hydrogen bond fastening the prestem (Asp45–Try118), which would ensure the release of the prestem. At the same time, this conformation would prevent the refolding of the stem following its release. The decrease in the hemolytic activity by the truncation of the amino latch may be partly caused by the inability to stably assemble into this conformation.

227 *3.5 Conclusion*

228 Based on the crystal structure analysis and mutation analysis, a dynamic pore formation
229 mechanism of α-HL was revealed. The prestem is fastened by a key hydrogen bond between Asp45
230 and Try118 in monomer, and the N-terminal amino latch released upon assembly destroys the key
231 hydrogen bond to release the prestem. During these processes, the hydrophobic interaction by the
232 N-terminal amino latch acts as key role. The β-barrel is formed by two-step manner as observed for
233 the previously reported staphylococcal two-component PFTs. The upper extaramembrane half is
234 formed in the prepore state, and the transmembrane region is inserted into the membrane to form a
235 pore, which completes the pore formation.

236

237

238 ## Acknowledgment

239 X-ray diffraction experiments were performed at Photon Factory and SPring-8 under
240 proposals 2012G515/2014G022 and 2012A1179/2012B1215/2013A1115/2015A1117, respectively.
241 This work was supported by Grants-in-Aid from the Ministry of Education, Science, Sports and
242 Culture of Japan (Y. T.).

243

244 ## Figure Legends

245 **Fig. 1 Crystals of α-hemolysin H35A monomer** (A) The overall structure of the α-HL monomer

(left) and protomer of the pore (right). The amino latch, prestem, cap, and rim are colored blue, orange, green, and magenta, respectively. Loop-A in the monomer is shown in red. The disordered region of the prestem is shown as an orange dotted line. (B) Interaction between the Loop-A and prestem through a hydrogen bond between Asp45 and Tyr118. Asp45 and Tyr118 are shown as sticks. The hydrogen bond is shown as a red dotted line. Colors of the cartoon correspond to Fig. 1A. (C) Comparison of the monomeric structures of LukF and LukD (stereo view). For clarity, the amino latch and prestem, which show marked structural differences between the three proteins, are highlighted, and the cap and rim are all colored white.

Fig. 2 Hemolytic activity and erythrocyte binding activity of mutants. (A) Relative hemolytic activity of wild-type α-HL (WT), Y118F, ΔN14, and WR for rabbit erythrocytes. (B) Relative binding amount of mutant proteins for the rabbit erythrocytes membrane. The graphs show average values from three individual experiments and the corresponding SD. (C) Heptamer complex formation of wild-type α-HL and WR mutant on rabbit erythrocyte membrane. Samples treated with 1% SDS at 100˚C or 20˚C were analyzed by Western blotting (shown as 100 and 20, respectively). Bands for monomer and complex form were indicated by white and black triangle, respectively.

Fig. 3 Structure of α-HL-WR mutant. (A) Tube model of the overall structure of heptameric α-HL-WR, which is colored according to the B-factor value, from blue at 35 $Å^2$ to red at 110 $Å^2$. The

265 width of the tube also corresponds to the B-factor. (B) Stereo representation of 2Fo–Fc electron
266 density map of the β-barrel contoured at 1.2 σ. Cα trace of the whole β-barrel structure is also shown.
267
268 **Fig. 4 Steric hindrance of the amino latch** (A) Stereo representation of the monomer superposed
269 on a protomer of the pore. Amino latch of the monomer and pore are shown as blue and green,
270 respectively. Prestem and stem are shown as yellow and red, respectively. The cap domain of the
271 monomer and pore are shown as white and pale blue, respectively. For clarity, the top of the
272 protruding stem is truncated. (B) Stereo representation of monomers aligned as two adjacent
273 protomers in the pore. The amino latch of each monomer is colored blue and green. The prestems are
274 colored red and yellow. The cap and rim of each protomer are shown in white and pale blue.
275
276 **Fig. 5 Hydrophobic interaction of the amino latch in the monomer (A) and in the pore (B)**
277 Residues participating in the interaction are shown as yellow sticks. (A) Domain colors correspond to
278 those in Fig. 1A. (B) The cartoon is colored according to the protomer. Sticks are colored according
279 to the protomer; the yellow and red residues are derived from blue and green protomers, respectively.
280
281 **Supplementary Fig. S1 Sequence alignment of α-HL and other staphylococcal PFTs**
282

Table 1 Data collection and refinement statistics

	α-HL-H35A (4YHD)	α-HL-WR (4P24)
Data collection		
Beamline	Photon Factory BL5A	Photon Factory BL17A
Space group	$P2_1$	$P4_12_12$
Cell dimensions		
a, b, c (Å)	75.9, 128.9, 135.3	170.1, 170.1, 202.9
α, β, γ (°)	90.0, 91.6, 90.0	90, 90, 90
Wavelength (Å)	1.0	0.98
Resolution (Å) [a]	37.4–2.80 (2.90–2.80)	48.6-3.10 (3.21-3.10)
No. of total/unique reflections	222,318/61,440 (25,460/7,895)	446,837/54,499 (44,367/5,383)
R_{sym} (%) [a, b]	12.1 (52.7)	20.54 (99.13)
Completeness (%) [a]	95.8 (76.7)	99.99 (99.98)
Multiplicity [a]	3.6 (3.2)	8.2 (8.2)
Average $I/\sigma(I)$ [a]	10.00 (2.13)	10.8(2.13)
Refinement		
Resolution (Å)	37.4–2.80	48.6-3.10
R_{work}/R_{free}	0.215/0.263	0.219/0.245
No. of atoms		
Protein	13499	16232
Ligand/ion	5	104
B-factors (Å^2)		
Protein	40.1	60.7
Ligand/ion	34.3	101.4
r.m.s.d.		
Bond lengths (Å)	0.004	0.005
Bond angles (°)	0.78	1.04

a Values in parentheses correspond to the highest resolution shell.

b $R_{merge} = \Sigma_h \Sigma_i |I_{h,i} - \langle I_h \rangle| / \Sigma_h \Sigma_i |I_{h,i}|$, where $\langle I_h \rangle$ is the mean intensity of a set of equivalent reflections.

References

Adams, P.D., Afonine, P.V., Bunkoczi, G., Chen, V.B., Davis, I.W., Echols, N., Headd, J.J., Hung, L.W., Kapral, G.J., Grosse-Kunstleve, R.W., McCoy, A.J., Moriarty, N.W., Oeffner, R., Read, R.J., Richardson, D.C., Richardson, J.S., Terwilliger, T.C., Zwart, P.H., 2010. PHENIX: a comprehensive Python-based system for macromolecular structure solution. Acta crystallographica. Section D, Biological crystallography 66, 213-221.

Emsley, P., Lohkamp, B., Scott, W.G., Cowtan, K., 2010. Features and development of Coot. Acta crystallographica. Section D, Biological crystallography 66, 486-501.

Jayasinghe, L., Miles, G., Bayley, H., 2006. Role of the amino latch of staphylococcal alpha-hemolysin in pore formation: a co-operative interaction between the N terminus and position 217. J Biol Chem 281, 2195-2204.

Kabsch, W., 2010. Xds. Acta Crystallogr D Biol Crystallogr 66, 125-132.

Kaneko, J., Kamio, Y., 2004. Bacterial two-component and hetero-heptameric pore-forming cytolytic toxins: structures, pore-forming mechanism, and organization of the genes. Biosci Biotechnol Biochem 68, 981-1003.

Kaneko, J., Ozawa, T., Tomita, T., Kamio, Y., 1997. Sequential binding of Staphylococcal gamma-hemolysin to human erythrocytes and complex formation of the hemolysin on the cell surface. Biosci Biotechnol Biochem 61, 846-851.

Kawate, T., Gouaux, E., 2003. Arresting and releasing Staphylococcal alpha-hemolysin at

306 intermediate stages of pore formation by engineered disulfide bonds. Protein Sci 12, 997-1006.
307 McCoy, A.J., Grosse-Kunstleve, R.W., Adams, P.D., Winn, M.D., Storoni, L.C., Read, R.J., 2007.
308 Phaser crystallographic software. J Appl Crystallogr 40, 658-674.
309 Nguyen, V.T., Higuchi, H., Kamio, Y., 2002. Controlling pore assembly of staphylococcal
310 gamma-haemolysin by low temperature and by disulphide bond formation in double-cysteine LukF
311 mutants. Mol Microbiol 45, 1485-1498.
312 Sugawara, T., Yamashita, D., Tanaka, Y., Kaneko, J., Kamio, Y., Tanaka, I., Yao, M., 2013.
313 Preliminary X-ray crystallographic study of staphylococcal alpha-haemolysin monomer. Acta
314 crystallographica. Section F, Structural biology and crystallization communications 69, 868-870.
315 Tanaka, Y., Hirano, N., Kaneko, J., Kamio, Y., Yao, M., Tanaka, I., 2011. 2-Methyl-2,4-pentanediol
316 induces spontaneous assembly of staphylococcal α-hemolysin into heptameric pore structure. Protein
317 Science 20, 448-456.
318 Walker, B., Bayley, H., 1995. Key residues for membrane binding, oligomerization, and pore
319 forming activity of staphylococcal alpha-hemolysin identified by cysteine scanning mutagenesis and
320 targeted chemical modification. J Biol Chem 270, 23065-23071.
321 Walker, B., Braha, O., Cheley, S., Bayley, H., 1995. An intermediate in the assembly of a
322 pore-forming protein trapped with a genetically-engineered switch. Chem Biol 2, 99-105.
323 Yamashita, D., Sugawara, T., Takeshita, M., Kaneko, J., Kamio, Y., Tanaka, I., Tanaka, Y., Yao, M.,
324 2014. Molecular basis of transmembrane beta-barrel formation of staphylococcal pore-forming

toxins. Nat Commun 5, 4897.

Yamashita, K., Kawai, Y., Tanaka, Y., Hirano, N., Kaneko, J., Tomita, N., Ohta, M., Kamio, Y., Yao, M., Tanaka, I., 2011. Crystal structure of the octameric pore of staphylococcal gamma-hemolysin reveals the beta-barrel pore formation mechanism by two components. Proceedings of the National Academy of Sciences of the United States of America 108, 17314-17319.

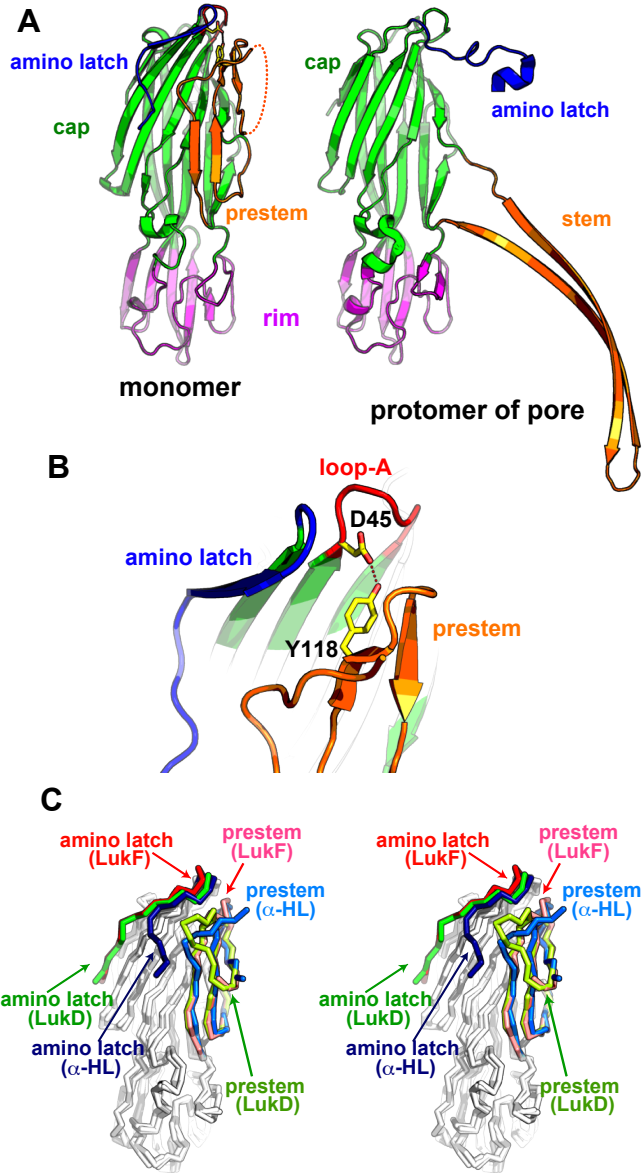

Fig. 1 (Sugawara et al.)

A

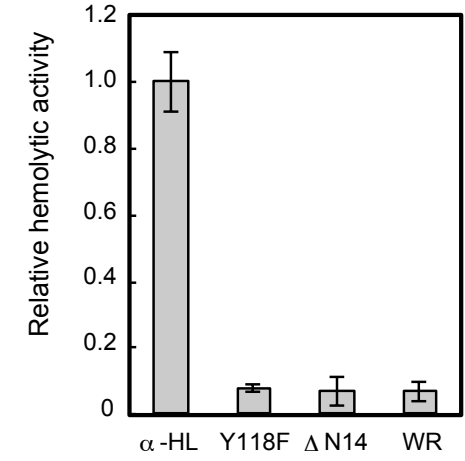

B

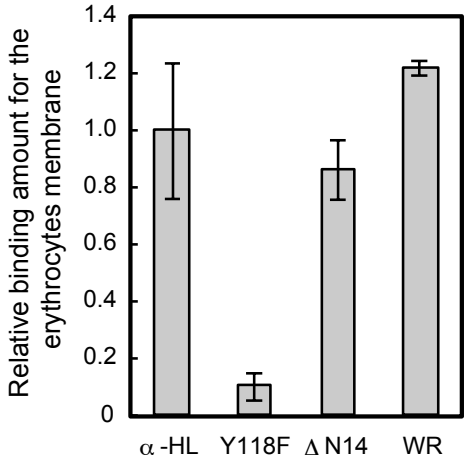

C

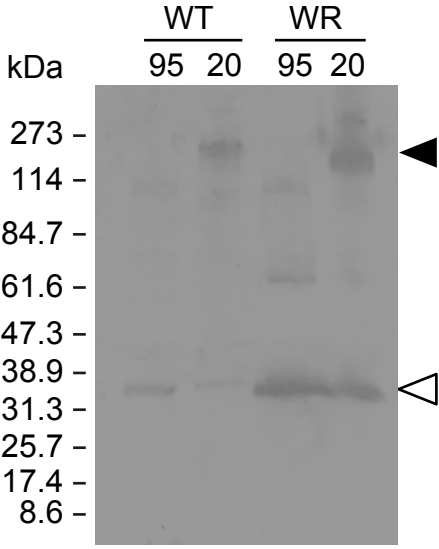

Fig. 2 (Sugawara et al.)

A

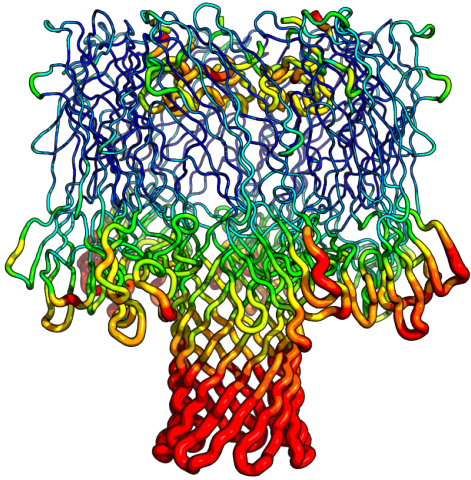

B

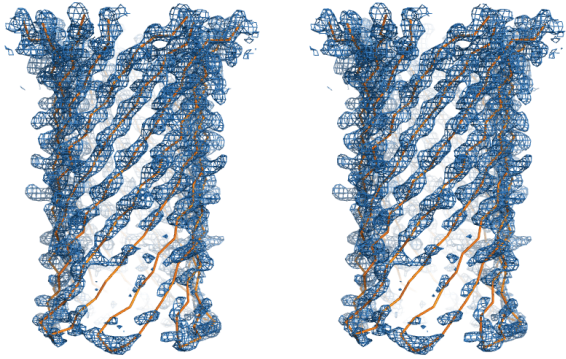

Fig. 3 (Sugawara et al.)

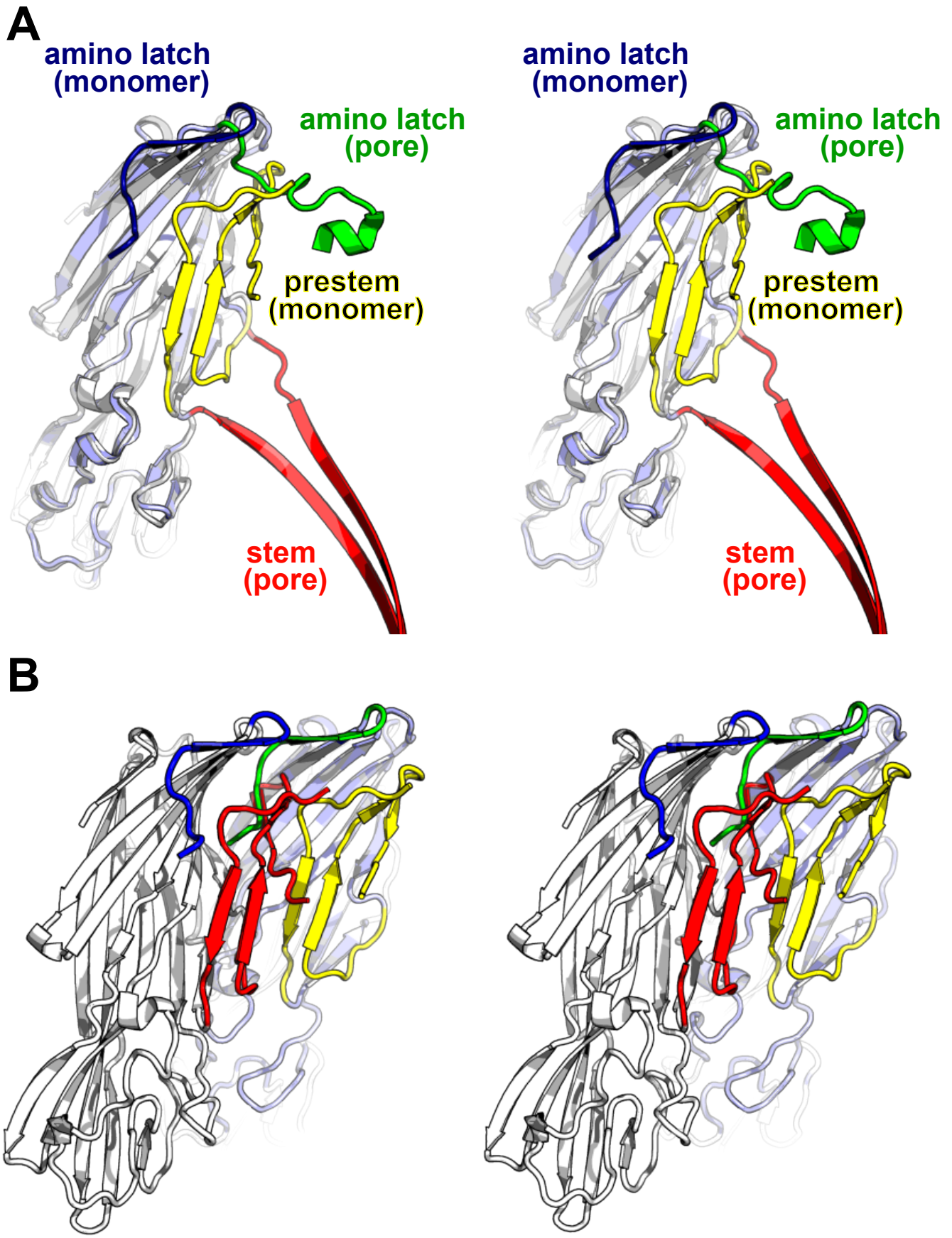

Fig. 4 (Sugawara et al.)

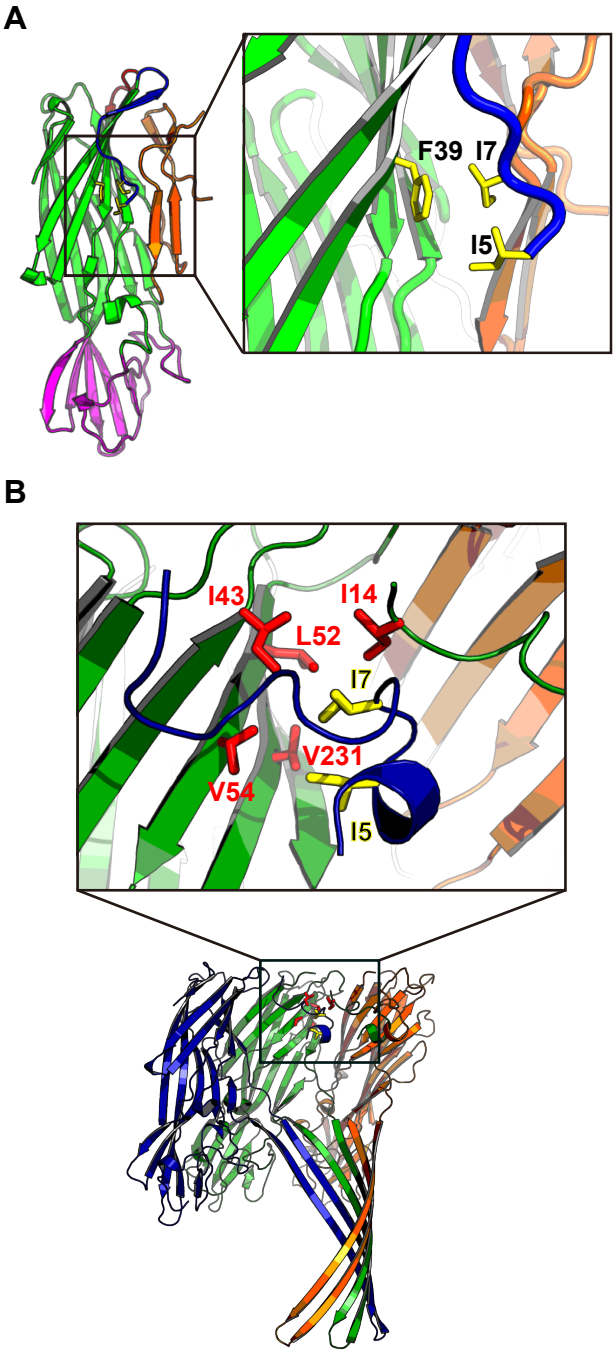

Fig. 5 (Sugawara et al.)

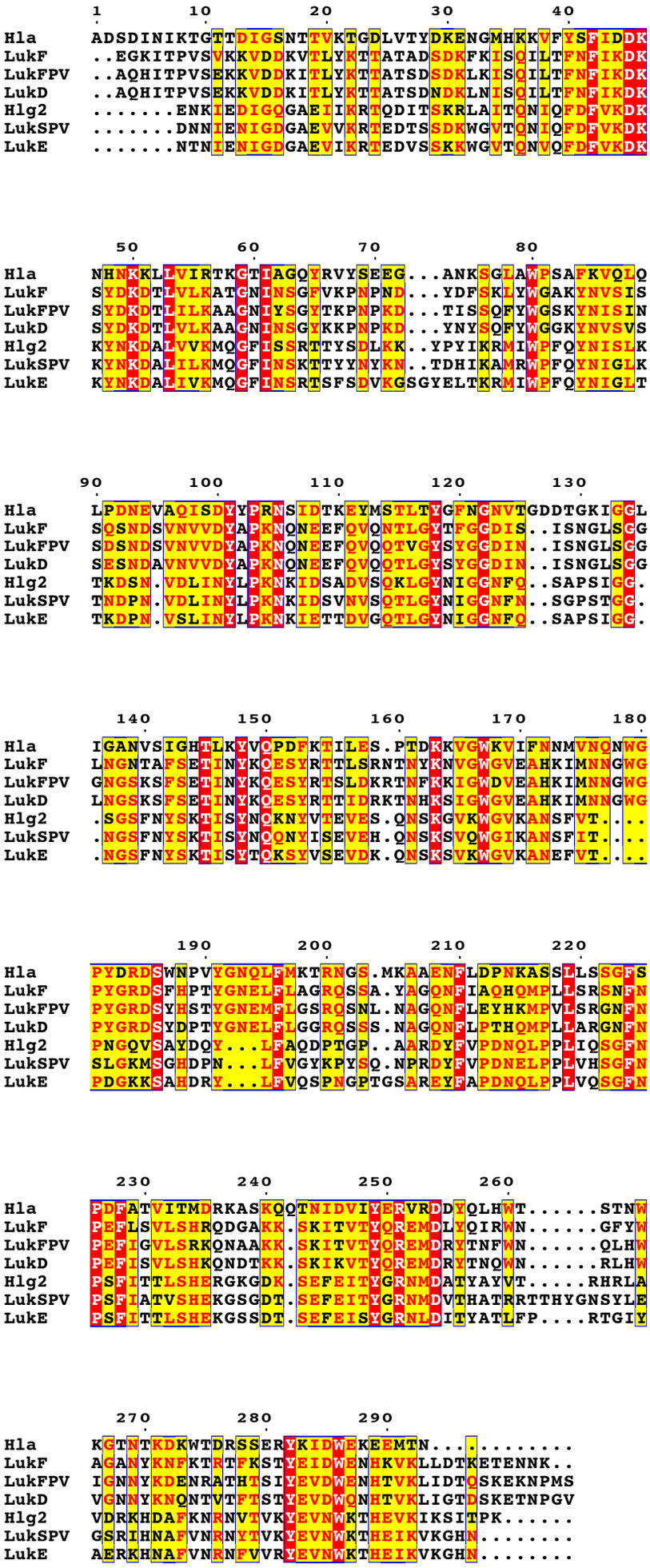

Supplementary Fig. S1 (Sugawara et al.)